



## PREPARATION AND CHARACTERIZATION OF ACTIVATED CARBON FROM DATE PALM (*Phoenix dactylifera*) SEEDS

\*Abdulkarim, M., Ibrahim, I. L., Mohammed, M. and Musah, M.

DeDepartment of Chemistry, Ibrahim Badamasi Babangida University Lapai, Nigeria

\*Corresponding authors' email: [mabdulkarim240@gmail.com](mailto:mabdulkarim240@gmail.com)

### ABSTRACT

In this study, agricultural waste (date seeds) were used to produce activated carbon in an oxygenated environment. The produced activated carbon was characterised. The HRSEM showed mesoporous structural morphology, which exhibited a surface area of 54.53 m<sup>2</sup>/g, pore size of 10.34 nm and pore volume of 0.1256 cc/g. The EDX spectrum revealed the presence of C and O as the major elemental compositions in the activated carbon. The FTIR spectrum indicated the presence of OH, C=C, C=O and C-H at absorption bands of 3400, 2900, 1650, and 1300 cm<sup>-1</sup>, respectively. The diffractogram of the activated carbon revealed graphitic carbon 2θ peaks of 22° and 43° which are related to (002) and (100) plane, respectively. The conversion of agricultural waste to activated carbon possessing these unique properties could serve as a promising and low-cost adsorbent for the removal of toxic pollutants from industrial wastewater.

**Keywords:** Carbonised, Surface area, Low-cost, Adsorbent

### INTRODUCTION

Activated carbon is an appropriate adsorbent for wastewater treatment because of its favourable attributes (Vakili *et al.*, 2023). It can be utilized in numerous applications where there is a need to eliminate dangerous organic substances and improve the absorbency of odours and flavours, making it more versatile than other technologies (Nabavi *et al.*, 2022). Activated carbon is an extremely efficient adsorbent due to its surface area and microporous nature.

Activated carbon can be made from different kinds of low-cost and agriculturally obtained materials like palm residue, corn cobs, apricot stones, and rice husks (Ani *et al.*, 2020). Date palm waste, which contains a significant amount of carbon, can be utilized to produce activated carbon (Nayl *et al.*, 2017). A number of scientists have successfully eliminated pollutants by utilizing activated carbon produced from biomass waste (Sun *et al.*, 2016).

### MATERIALS AND METHODS

#### Sample Collection

The biomass sampling was carried out as described by (Varsani *et al.*, 2022). This study utilized date palm seeds to produce activated carbon, which was then used to treat wastewater from the textile industry (Subki *et al.*, 2020).

The date seeds were obtained from Minna central mosque surrounding in Minna, Niger State, Nigeria. The seeds were washed multiple times with distilled water and dried in the sun completely. After that, the seeds were ground in a high speed rotary mill and sifted through a mesh with a number 100. Finally, the resulting powder was stored in an airtight container for future use.

### Sample Preparation

#### Carbonization

Five clean and pre-weighed crucibles were each filled with five grams of the pre-treated sample. These crucibles were placed in a muffle furnace at 400 °C for 20 minutes and then cooled in iced water. The excess water was removed with filter paper, and the sample was dried at room temperature before being washed with distilled water. This washing process was repeated multiple times until a significant amount of carbonized sample was obtained. The carbonized samples were then washed with 0.1 M HCl to remove ash, followed by further washing with distilled water until reaching a pH of 7 to eliminate acid residue. The washed samples were left to air dry at room temperature (Reza *et al.*, 2020).

#### Activation

The carbonated samples were activated by mixing 1 gram of the sample with 1 cubic centimeter of the activating agent (1M H<sub>3</sub>PO<sub>4</sub>) in a 1:1 ratio. The samples were then soaked in the activating agent and promptly placed in a furnace for activation at a high temperature of 550 °C for a duration of 10 minutes.

The activated samples were taken out and cooled in cold water to avoid ash contamination, then washed well with 0.1 M HCl to remove ash from the activated carbon surface. Next, they were washed with hot water and then rinsed with distilled water until pH 7 was achieved. The samples were filtered using filter paper and air-dried, and this process was repeated until a significant amount of activated carbon was obtained (Reza *et al.*, 2020).

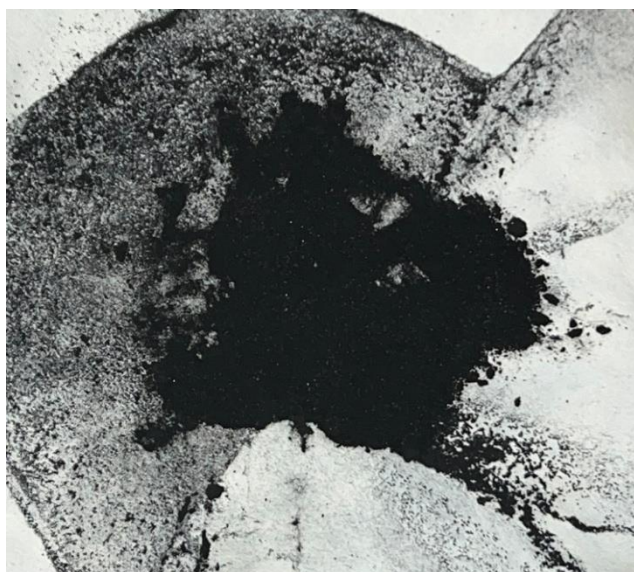


Figure 1: Date seeds activated carbon

### Scanning Electron Microscope (SEM)

First, the sample was prepared by mounting it on a specimen grid, and then coating it with a thin layer of metal to prevent charging and enhance conductivity.

Next, the sample was inserted into the SEM (FEG 450; United State of America) instrument, which was calibrated according to the manufacturer's instructions. The instrument produces a focused beam of electrons, which was scanned across the sample in a raster pattern.

The resulting secondary electrons were detected and used to produce a high-resolution image of the sample's surface morphology, with a typical magnification range of 10-100,000 times.

The SEM image was then analyzed to examine the sample's surface features, such as texture, topography, and particle size and shape. The image was typically recorded in digital format and may be processed using image analysis software to enhance contrast and resolution.

### Brunauer Emmett Teller (BET)

First, the sample was prepared by degassing it at 300°C and vacuum to remove any adsorbed impurities.

Next, the sample was placed in a sample cell and attached to the BET (BQ50-IJ; United State of America) instrument, which was calibrated according to the manufacturer's instructions.

The instrument then measures the amount of gas (typically nitrogen) adsorbed onto the sample surface at various relative pressures, using a static or dynamic adsorption technique.

The resulting adsorption isotherm was then analyzed using the BET equation to determine the specific surface area of the sample, typically expressed in units of square meters per gram (m<sup>2</sup>/g).

Finally, the results are reported in a table or graph, including the specific surface area, pore size distribution.

### Fourier-transform Infrared Spectroscopy (FTIR)

First, the sample was prepared by grinding it into a fine powder. The sample was then placed on a sample holder, ensuring good contact and minimal interference.

Next, the FTIR (FTIR-8400S; Japan) instrument was calibrated according to the manufacturer's instructions, and the sample was inserted into the instrument. The instrument

scans the sample over a range of wavenumbers (typically 4000 - 400 cm<sup>-1</sup>) using an interferometer and detector.

The resulting interferogram was then converted into a spectrum using Fourier transform, and the spectrum was plotted as absorbance or transmittance vs. wavenumber.

The FTIR spectrum was then analyzed to identify the functional groups and molecular structures present in the sample, using reference spectra from the instrument's database. The peak positions, intensities, and shapes were used to determine the sample's molecular composition and structure.

### Energy Dispersive X-ray (EDX)

First, the sample was prepared by coating it with a thin layer of carbon to prevent charging. The sample was then inserted into the EDX (EDX 800; China) instrument, which was calibrated according to the manufacturer's instructions.

Next, the sample was bombarded with a focused beam of electrons, causing the emission of X-rays characteristic of the elements present. The energy and intensity of these X-rays were measured using a detector, and the resulting spectrum was plotted as intensity vs. energy.

The EDX spectrum was then analyzed to identify the elemental composition of the sample, using reference spectra from the instrument's database or other sources. The relative intensities of the peaks are used to determine the elemental concentrations, typically expressed as weight percent (wt%) or atomic percent (at%).

### X-ray diffraction analysis (XRD)

First, the sample was prepared by grinding it into a fine powder and ensuring its homogeneity. Then, the powdered sample was mounted onto a sample holder, ensuring even spread and packing.

Next, the XRD (DW-XRD-2700A; China) instrument was set up by aligning the X-ray beam, adjusting the detector, and calibrating the instrument with a standard reference material. Data collection was initiated by selecting the desired measurement parameters, such as the range of angles to be scanned and the step size. The XRD instrument rotates the sample holder while measuring the intensity of diffracted X-rays at different angles.

The collected data was then analyzed using XRD software or other analytical tools. The software processes the diffraction patterns and generates an XRD pattern or diffractogram.

Peak identification was performed by comparing the peaks in the XRD pattern to known patterns from a database. These peaks represent the diffraction of X-rays by the crystal lattice of the sample.

The XRD pattern was interpreted to determine the crystal structure, phase composition, crystallinity, and other properties of the sample.

This involves analyzing peak positions, peak intensities, and peak shapes.

#### Thermogravimetric Analysis (TGA)

First, the TGA (PinAAcle™500; United State of America) instrument was set up by calibrating the balance and ensuring that the furnace and gas flow are appropriately controlled.

The sample was prepared by weighing 5 mg and placing it in a sample crucible. The crucible was then placed on the balance inside the TGA instrument.

The TGA analysis begins by heating the sample at a constant rate, in a controlled atmosphere of nitrogen. The temperature range and heating rate was set at 10 °C / min.

As the sample was heated, the TGA instrument continuously measures the weight of the sample as a function of temperature or time.

The balance detects any changes in weight, which are attributed to the sample undergoing thermal decomposition, evaporation, or other chemical or physical transformations.

The TGA instrument records the weight change data and plots it as a thermogram, which shows the weight loss or gain as a function of temperature or time.

The thermogram was analyzed to determine various characteristics of the sample, such as the onset temperature of

decomposition or volatilization, the rate of weight loss, and the total amount of weight change.

## RESULTS AND DISCUSSION

### TGA Curve

The TGA curve of activated carbon as presented in Fig. 1 exhibits distinct weight loss events corresponding to different thermal decomposition processes. The onset temperature of 342.75 °C indicates the point at which the removal of volatile substances begins from the activated carbon structure. Volatile substances are relatively low boiling points that are easily vaporized upon heating. These may include residual solvents, adsorbed gases, or other volatile contaminants present in the activated carbon. The production of high-performance activated carbons from hemicellulose residues of poplar underscores the significance of activated carbon in adsorption processes, shedding light on its role in eliminating volatile substances (He *et al.*, 2023). As the temperature increases beyond the onset temperature, these volatile substances start to desorb and evaporate from the activated carbon matrix. This weight loss event is typically observed as a gradual decrease in weight on the TGA curve, reflecting the gradual removal of volatile components. Organic matter present in activated carbon can originate from various sources, including carbonaceous precursors used in the activation process or organic contaminants adsorbed onto the surface. The fact that this degradation step occurs in a single step suggests that the organic matter is relatively homogenous in composition or that it undergoes a uniform decomposition process. The sharp weight loss observed on the TGA curve during this stage indicates rapid decomposition of the organic matter, resulting in the release of volatile products such as CO<sub>2</sub>, CO, and other gases.

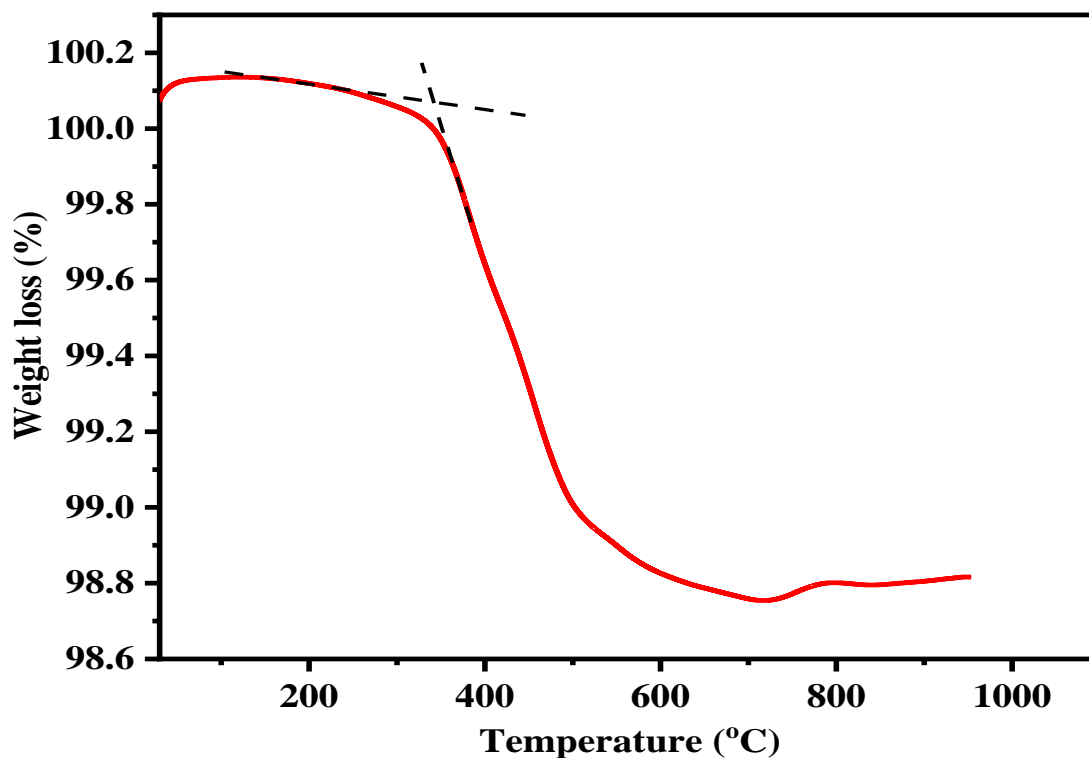


Figure 2: The TGA curve of activated carbon prepared from date seed

### EDX analysis

In Fig. 2. The carbon (C) is the primary constituent of activated carbon is the dominate the spectrum with strong peaks in the low-energy range. This peak appeared around 0.2-0.3 keV on the energy scale. The intensity of C peak reflects the amount of carbon present in the sample, providing quantitative information about its concentration as shown in Fig. 2. The presence of oxygen (O) could exists in various forms on the surface of activated carbon due to adsorption of atmospheric oxygen or functionalization during activation processes. This peak occurs at slightly higher energies, around 0.5-0.7 keV. The intensity and position of this peak indicates the extent of oxidation or functionalization of the carbon

surface. Studies have identified the presence of oxygen-containing functional groups on activated carbon surfaces, such as carbonyl, ester, carboxyl, and hydroxyl groups, which act as active sites for adsorption processes (Cho *et al.*, 2008; Shen *et al.*, 2019). These functional groups play a crucial role in influencing adsorption processes and various reactions involving carbon surfaces. The presence of silicon (Si), typically around 1-1.5 keV might originate from impurities in the raw materials used for carbon activation or from surface modifications during synthesis processes. The intensity of silicon peaks can provide information about the extent of silicon incorporation or contamination in the activated carbon structure.

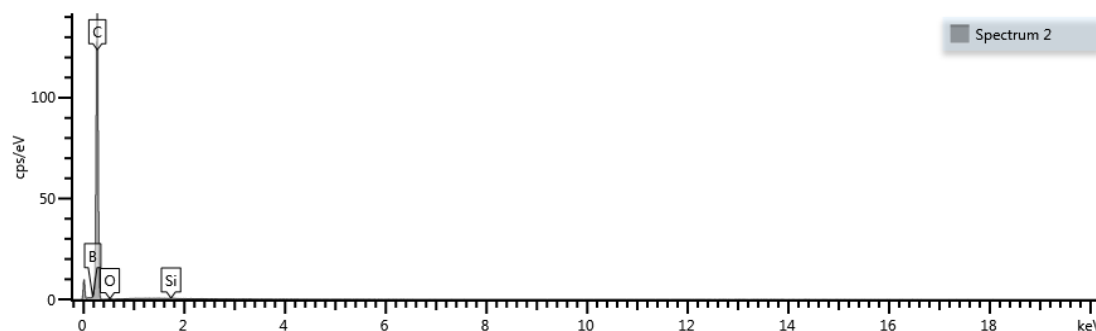


Figure 3: EDX of ACDS

### Brunauer emmett teller (BET) Analysis of Activated Carbon from Date Seeds

This analysis provided critical data on the surface area, pore volume, and pore size of the activated carbon, which are key parameters influencing its adsorption capacity.

#### Surface Area

The BET analysis revealed that the activated carbon derived from date seeds has an average surface area of 54.5286 m<sup>2</sup>/g. This surface area is relatively low when compared to commercially available activated carbons, which typically have surface areas ranging from 500 to 1500 m<sup>2</sup>/g. The lower surface area suggests that the date seed activated carbon may have a limited capacity for adsorbing contaminants.

#### Pore Volume

The average pore volume of the date seed activated carbon was found to be 0.12598 cc/g. Pore volume represents the total space within the adsorbent material that can accommodate adsorbate molecules. A pore volume of 0.12598 cc/g is indicative of a moderate capacity for holding contaminants. This volume is relatively good for an activated

carbon produced from natural materials, implying that the date seed activated carbon has a substantial number of pores capable of trapping and holding molecules.

#### Pore Size

The BET analysis showed that the date seed activated carbon has an average pore size of 103346 Å (103.346 nm). This pore size classifies the material as macroporous (pores larger than 50 nm). The large pore size is advantageous for the adsorption of larger organic contaminants, which are typically present in wastewater. However, it may limit the adsorbent's efficiency for smaller organic molecules that also contribute to these measures. Generally, mesoporous materials (with pore sizes between 2-50 nm) are considered more effective for adsorbing a broader range of molecules due to their optimal balance of surface area and accessibility.

To enhance the adsorbent's performance, strategies such as chemical or physical activation could be employed to increase its surface area and optimize pore size distribution. Such modifications could significantly improve its capacity to adsorb a broader range of contaminants, making it more competitive with commercial activated carbons.

Table 1: Summary of BET analysis

Activation Temperature (°C)	BET surface area(m <sup>2</sup> /g)	Total pore volume (cm <sup>3</sup> /g)	Pore Size(Å)
550	54.5286	0.12598	103,346

### Fourier-transform infrared spectroscopy (FTIR)

In Fig. 3 the FTIR spectrum provides insights into the functional groups present on the surface of the activated carbon. Key absorption bands were observed at approximately 3400 cm<sup>-1</sup>, indicative of O-H stretching vibrations, suggesting the presence of hydroxyl groups. The peaks around 2900 cm<sup>-1</sup> are attributed to C-H stretching in aliphatic hydrocarbons, while strong peaks near 1700-1600 cm<sup>-1</sup> correspond to C=O stretching vibrations, highlighting the presence of carbonyl groups such as ketones, aldehydes, and carboxylic acids. These functional groups are critical for

adsorption processes, as they enhance the affinity for both polar and non-polar contaminants in wastewater.

Additional peaks between 1300-1000 cm<sup>-1</sup>, associated with C-O stretching vibrations, indicate the presence of ethers and alcohols, while the aromatic C=C stretching in the 1600 cm<sup>-1</sup> region suggests some degree of graphitization. The diversity of functional groups as revealed by FTIR supports the high adsorption efficiency of the activated carbon, making it suitable for removing a wide range of organic and inorganic pollutants.

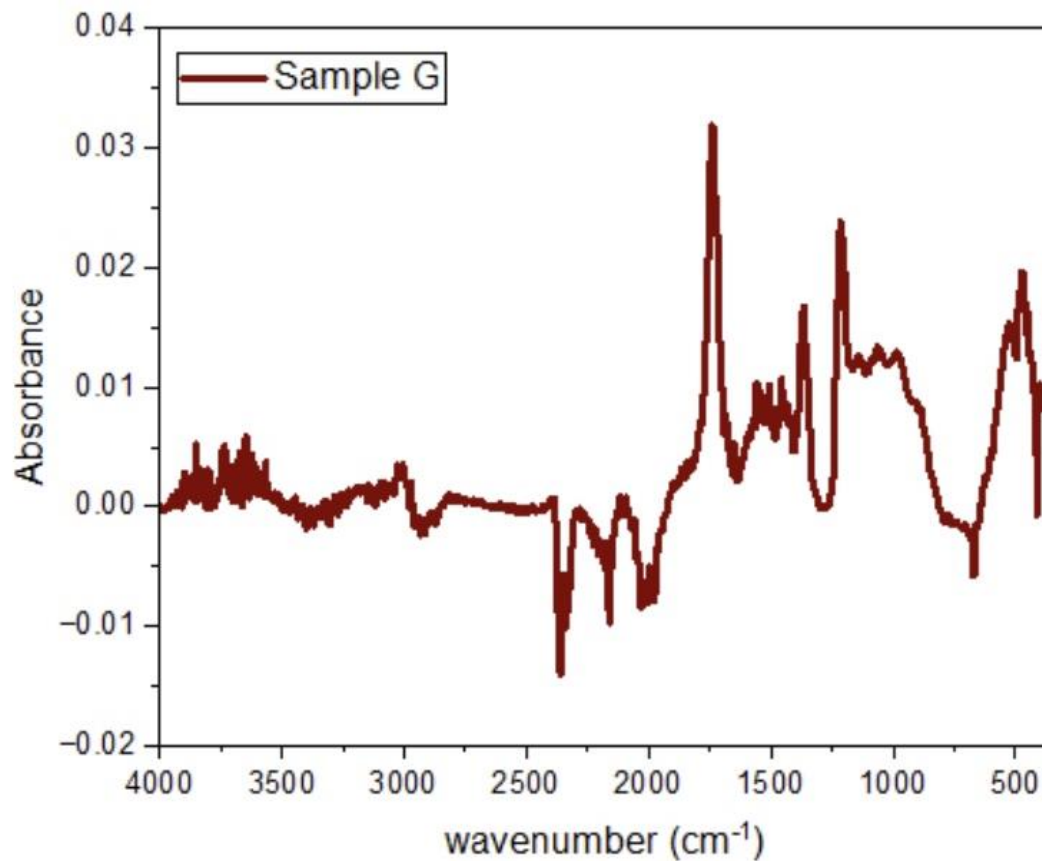


Figure 4: FTIR of ACDS

**X-ray diffraction analysis (XRD)**

The XRD pattern of the activated carbon shows broad peaks around  $22^\circ$  and  $43^\circ$   $2\theta$ , characteristic of amorphous carbon with some graphitic microcrystalline domains. The broad peak at  $22^\circ$  corresponds to the (002) plane of graphitic carbon, indicating some layered structures, while the peak at  $43^\circ$  is related to the (100) plane, confirming the presence of graphitic structures within the amorphous matrix (Mubari et al., 2022).

The predominantly amorphous nature, as evidenced by the broad peaks, suggests a high degree of disorder, which is beneficial for adsorption due to the extensive porosity and surface area. The presence of both amorphous and graphitic domains enhances the material's structural stability and adsorption capacity, as the graphitic regions provide mechanical strength and stability, while the amorphous regions contribute to a high surface area and porosity.

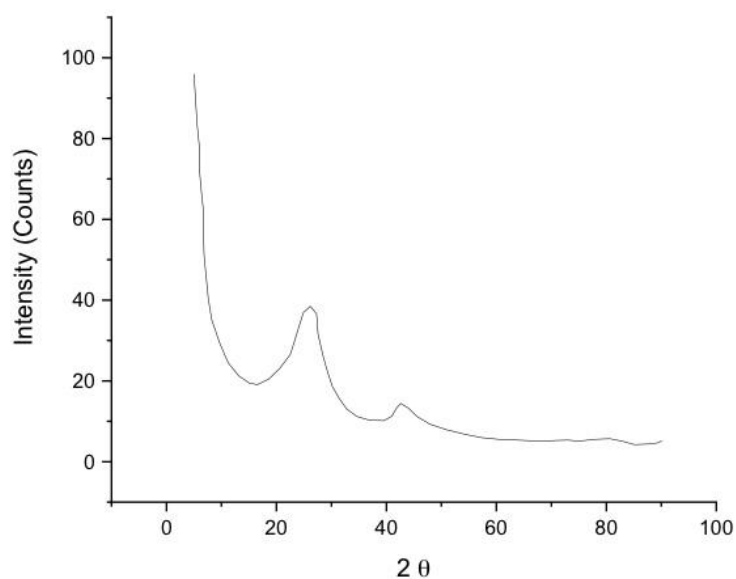


Figure 5: XRD of ACDS

### Scanning electron microscope (SEM)

The SEM images in Fig. 5 of the activated carbon produced from date seeds reveal a highly porous structure with irregular surface morphology, indicating the successful development of a large surface area. The high magnification images show a network of micropores and mesopores, essential for adsorption. The combined physical and chemical activation

processes facilitated the creation of an extensive pore structure, which is crucial for enhancing the adsorption capacity. The visible roughness and heterogeneity of the surface suggest a high degree of surface activation, which directly correlates with increased interaction sites for adsorbates (Chulliyil *et al.*, 2024).

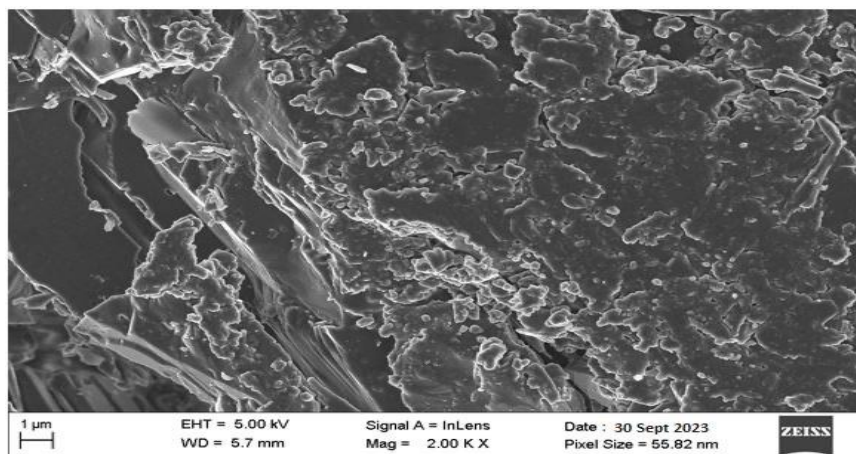


Figure 6: SEM image of ACDS

### CONCLUSION

It is varied from the obtained results that date palm (*Phoenix dactylifera*) seeds is a good agricultural by-product for the preparation of quality adsorbent material as it portray characteristics of a quality mesoporous activated carbon which can be used for adsorption purposes in applications such as gaseous pollutant adsorption, adsorbent of iodine, methylene blue and residual chlorine.

### REFERENCES

Ani, J. U., Akpomie, K. G., Okoro, U. C., Aneke, L. E., Onukwuli, O. D., & Ujam, O. T. (2020). Potentials of activated carbon produced from biomass materials for sequestration of dyes, heavy metals, and crude oil components from aqueous environment. *Applied Water Science*, 10(2), 69. <https://doi.org/10.1007/s13201-020-1149-8>.

Cho, H., Smith, B., Wnuk, J., Fairbrother, D., & Ball, W. (2008). Influence of surface oxides on the adsorption of naphthalene onto multiwalled carbon nanotubes. *Environmental Science & Technology*, 42(8), 2899-2905. <https://doi.org/10.1021/es702363e>.

Chulliyil, H. M., Hamdani, I. R., Ahmad, A., Al Shoaibi, A., & Chandrasekar, S. (2024). Enhanced moisture adsorption of activated carbon through surface modification. *Results in Surfaces and Interfaces*, 14, 100170. <https://doi.org/10.1016/j.rsurfi.2023.100170>.

He, J., Zhao, Y., Zhou, Y., & Wu, S. (2023). Preparation of high-performance activated carbons from hemicellulose vocs-extracted residues of poplar and their application in vocs removal. *Bioresources*, 18(2), 2874-2896. <https://doi.org/10.15376/biores.18.2.2874-2896>.

Mubari, P. K., Beguerie, T., Monthieux, M., Weiss-Hortala, E., Nzihou, A., & Puech, P. (2022). The X-ray, Raman and TEM signatures of cellulose-derived carbons explained. *C*, 8(1), 4. <https://doi.org/10.3390/c8010004>.

Nabavi, E., Sabour, M., & Dezvareh, G. A. (2022). Ozone treatment and adsorption with granular activated carbon for the removal of organic compounds from agricultural soil leachates. *Journal of Cleaner Production*, 335, 130312. <https://doi.org/10.1016/j.jclepro.2021.130312>.

Nayl, A. E. A., Elkhatab, R. A., El Malah, T., Yakout, S. M., El-Khateeb, M. A., Ali, M. M. S., & Ali, H. M. (2017). Adsorption studies on the removal of COD and BOD from treated sewage using activated carbon prepared from date palm waste. *Environmental Science and Pollution Research*, 24(28), 22284-22293. <https://doi.org/10.1007/s11356-017-9878-4>.

Reza, S., Yun, C. S., Afroze, S., Radenahmad, N., AbuBakar, M. S., Saidur, R., Taweekun, J. & Azad, A. K. (2020). Preparation of activated carbon from biomass and its applications in water and gas purification, a review. *Arab Journal of Basic and Applied Sciences*, 27(1), 208-238. <https://doi.org/10.1080/25765299.2020.1766799>.

Shen, F., Liu, J., Gu, C., & Wu, D. (2019). Roles of oxygen functional groups in hydrogen sulfide adsorption on activated carbon surface: a density functional study. *Industrial & Engineering Chemistry Research*, 58(14), 5526-5532. <https://doi.org/10.1021/acs.iecr.9b00507>.

Sun, Y., Li, H., Li, G., Gao, B., Yue, Q., & Li, X. (2016). Characterization and ciprofloxacin adsorption properties of activated carbons prepared from biomass wastes by H<sub>3</sub>PO<sub>4</sub> activation. *Bioresource Technology*, 217, 239-244. <https://doi.org/10.1016/j.biortech.2016.03.047>.

Subki, N. S., Akhir, N. M., Abdul Halim, N. S., & Nik Yusoff, N. R. (2020). COD Reduction in Industrial Wastewater Using Activated Carbon Derived from Wodyetia Bifurcata Fruit. *IOP Conference Series: Earth and Environmental Science*, 549(1), 012066. <https://doi.org/10.1088/1755-1315/549/1/012066>.

Vakili, A., Zinatizadeh, A. A., Rahimi, Z., Zinadini, S., Mohammadi, P., Azizi, S., Karami, A., & Abdulgader, M. (2023). The impact of activation temperature and time on the characteristics and performance of agricultural waste-based activated carbons for removing dye and residual COD from wastewater. *Journal of Cleaner Production*, 382, 134899. <https://doi.org/10.1016/j.jclepro.2022.134899>.

Varsani, V., Vyas, S. J., & Dudhagara, D. R. (2022). Development of bio-based material from the *Moringa oleifera* and its bio-coagulation kinetic modeling—A sustainable approach to treat the wastewater. *Heliyon*, 8(9), e10447. <https://doi.org/10.1016/j.heliyon.2022.e10447>.



©2024 This is an Open Access article distributed under the terms of the Creative Commons Attribution 4.0 International license viewed via <https://creativecommons.org/licenses/by/4.0/> which permits unrestricted use, distribution, and reproduction in any medium, provided the original work is cited appropriately.